# REPORT DOCUMENTATION PAGE

*Form Approved*
*OMB No. 0704-0188*



**PLEASE DO NOT RETURN YOUR FORM TO THE ABOVE ADDRESS.**

| 1. REPORT DATE *(DD-MM-YYYY)* | 2. REPORT TYPE | 3. DATES COVERED *(From - To)* |
|---|---|---|
| 2-22-2010 | Final | 01-01-2008 to 12-31-2010 |

**4. TITLE AND SUBTITLE**

YIP-08 - NANOPLASMONIC CATALYSIS FOR SYNTHETIC FUEL PRODUCTION

**5a. CONTRACT NUMBER**

FA9550-08-1-0019

**5b. GRANT NUMBER**

FA9550-08-1-0019

**5c. PROGRAM ELEMENT NUMBER**

**6. AUTHOR(S)**

Stephen B. Cronin

**5d. PROJECT NUMBER**

**5e. TASK NUMBER**

**5f. WORK UNIT NUMBER**

**7. PERFORMING ORGANIZATION NAME(S) AND ADDRESS(ES)**

University of Southern California
3737 Watt Way
Los Angeles, CA 90089

**8. PERFORMING ORGANIZATION REPORT NUMBER**

**9. SPONSORING/MONITORING AGENCY NAME(S) AND ADDRESS(ES)**

Air Force Office of Scientific Research
875 North Randolph Street
Suite 325, Rm 3112
Arlington, VA 22203

**10. SPONSOR/MONITOR'S ACRONYM(S)**

AFOSR

**11. SPONSOR/MONITOR'S REPORT NUMBER(S)**

AFRL-OSR-VA-TR-2012-0056

**12. DISTRIBUTION/AVAILABILITY STATEMENT**

A

**13. SUPPLEMENTARY NOTES**

**14. ABSTRACT**

Our objective is to assess whether catalytic enhancement can be achieved in the production of synthetic fuels by integrating plasmon resonant nanostructures with strongly catalytic materials. We seek a fundamental understanding of the basic mechanism underlying this enhancement with the ultimate goal of producing synthetic fuels, such as hydrogen, methane and methanol using visible illumination.

**15. SUBJECT TERMS**

SERS, plasmonics, nanogap, shadow mask, angle evaporation

| 16. SECURITY CLASSIFICATION OF: | | | 17. LIMITATION OF ABSTRACT | 18. NUMBER OF PAGES | 19a. NAME OF RESPONSIBLE PERSON |
|---|---|---|---|---|---|
| a. REPORT | b. ABSTRACT | c. THIS PAGE | | | Stephen Cronin |
| U | U | U | UU | 6 | 19b. TELEPHONE NUMBER *(Include area code)* 213-740-8787 |

Reset

**Standard Form 298** (Rev. 8/98)
Prescribed by ANSI Std. Z39.18

**FINAL PERFORMANCE REPORT**

***YIP: Nanoplasmonic Catalysis for Synthetic Fuel Production***

Prof Steve Cronin
University of Southern California

**Abstract:**

Our objective is to assess whether catalytic enhancement can be achieved in the production of synthetic fuels by integrating plasmon resonant nanostructures with strongly catalytic materials. We seek a fundamental understanding of the basic mechanism underlying this enhancement with the ultimate goal of producing synthetic fuels, such as hydrogen, methane and methanol using visible illumination.

**Objectives:**

- Fabricate arrays of metal nanostructures on top of and embedded in both active (e.g., $TiO_2$) and non-active metal oxide supports.
- Monitor the reaction rates of photocatalytic processes using mass spectrometry, gas chromatography, and potentiostatic electrochemistry while irradiating these plasmonic/catalytic nanostructures at their plasmon resonance frequency.
- Establish whether direct transfer of charge occurs between the plasmonic metal and the metal oxide semiconductor, by performing electromagnetic simulations of the plasmonic/catalytic nanostructures using the finite-difference time-domain (FDTD) method.
- Determine how doping affects the catalytic enhancement in the visible wavelength range, by comparing the catalytic activity of doped and undoped $TiO_2$.
- Establish an optimized method for producing strongly plasmonic arrays of nearly touching metal nanoparticles.

**Status of Effort:**

Significant progress has been made in each of the primary objectives listed above. We have successfully demonstrated plasmonic enhancement of several photochemical processes (e.g., water splitting, methyl orange decomposition, and CO oxidation) by integrating strongly plasmonic metal nanostructures with strongly catalytic metal oxide semiconductors. We have achieved enhancement factors as high as 66-fold, however, the overall photoconversion efficiencies were still quite low in the visible wavelength range. Our theoretical modeling of this system indicates that enhancement factors much larger than this can be achieved if the nanoparticle geometries can be optimized.

**Personnel Supported:**

Prof. Stephen Cronin (PI)
Wei Hsuan Hung (PhD student)
Prathamesh Pavaskar (PhD student)

Wei Hsuan Hung will be graduating with his PhD this spring 2011 semester. Thesis entitled “Plasmon Resonant Enhancement of Catalytic Processes and Solar Energy Conversion.”

**Peer Reviewed Journal Publications:**

Zuwei Liu, Wenbo Hu, Prathamesh Pavaskar, Mehmet Aykol, and Stephen B. Cronin, *Plasmon Resonant Enhancement of Photocatalytic Water Splitting Under Visible Illumination*, **Nano Letters**, in press (2011).

Wenbo Hou, Zuwei Liu, Prathamesh Pavaskar, Wei Hsuan Hung, and Stephen B. Cronin, *Plasmonic Enhancement of Photocatalytic Decomposition of Methyl Orange Under Visible Light*, **Journal of Catalysis**, in press (2011).

Wei Hsuan Hung, Mehmet Aykol, David Valley, and Stephen B. Cronin, *Plasmon Resonant Enhancement of Carbon Monoxide Catalysis*, **Nano Letters**, 10, 1314 (2010).

Theiss, Jesse; Pavaskar, Prathamesh; Echternach, Pierre; Cronin, Stephen, *Plasmonic Nanoparticle Arrays with Nanometer Separation for High-Performance SERS Substrates*, **Nano Letters**, 10, 2749 (2010).

Zuwei Liu, Wei Hsuan Hung, Mehmet Aykol, David Valley and Stephen B Cronin, *Optical manipulation of plasmonic nanoparticles, bubble formation and patterning of SERS aggregates*, **Nanotechnology**, 21, 105304 (2010).

Prathamesh Pavaskar and Stephen B. Cronin, *Iterative optimization of plasmon resonant nanostructures*, **Applied Physics Letters**, 94, 254102 (2009).

Wei Hsuan Hung, I-Kai Hsu, Adam Bushmaker, Rajay Kumar, Jesse Theiss, and Stephen B. Cronin, *Laser Directed Growth of Carbon-Based Nanostructures by Plasmon Resonant Chemical Vapor Deposition*, **Nano Letters,** 8, 3278 (2008).

**Presentations at Conferences and Meetings:**

Wei-Hsuan Hung "Laser-induced Plasmonic Catalysis for Synthesis Carbon-based Nanostructures" Materials Research Society Spring Meeting, San Francisco, California, April 27, 2011.

P. C. Pavaskar, "Optimization of Plasmonic Nanostructures", Quantum Sensing and Nanophotonic Devices VIII, SPIE Photonics West, San Francisco, CA, January 24, 2011.

S. B. Cronin, "Plasmonic Enhancement of Photocatalytic Processes" Gordon Research Conference on Plasmonics, Colby College, Waterville, ME, June 17, 2010.

W. Hou, "Plasmonic Enhancement of Photocatalytic Reactions" 2010 Materials Research Society Fall Meeting, Boston, MA, Nov 29, 2010.

Jesse Theiss, Prathamesh Pavaskar, Pierre M. Echternach, and Stephen B. Cronin, "Fabrication and SERS Characterization of Plasmonically Coupled Nanoparticles With Nanometer Separation" American Physical Society March Meeting 2010, Portland, OR, March 15-19, 2010.

P. C. Pavaskar, "Iteratively Optimized Nonperiodic Plasmon Resonant Nanostructures", Quantum Sensing and Nanophotonic Devices VII, SPIE Photonics West, San Francisco, CA, January 26, 2010.

**Poster Presentations:**

P. C. Pavaskar, "Exploring optimized configurations of plasmonic nanoparticles", Metallic Nanostructures and Their Optical Properties VIII, SPIE Optics + Photonics, San Diego, CA, United States, August 2, 2010

P. C. Pavaskar, "Towards optimized geometries of plasmon resonant nanostructures", Symposium M: Resonant Optical Antennas--Sensing and Shaping Materials, 2010 MRS Fall Meeting, Boston, MA, United States, December 1, 2010

**Broader Impact:**

The fundamental understanding of catalytic enhancement gained in this research effort has provided a new path toward resolving the photon absorption/electron diffusion path length mismatch that has made photovoltaics and direct photocatalysts far too expensive to find broad applicability in our energy infrastructure. For photocatalysis, this area is especially exciting because it presents a possible route to direct solar-to-fuel production. Though this work is far from a commercial reality, the “basic science” understanding gain is needed in order to obtain sufficient control over the proposed processes. Given the complex chemistry and condensed matter physics involved, this basic scientific understanding is crucial, as Edisonian approaches are likely to fail.

## INTRODUCTION

**Solar Utilization:** Solar energy presents a promising alternative as an abundant, largely untapped resource. The amount of energy striking the Earth from sunlight in one hour ($4.3 \times 10^{20}$ J) is more than the total energy consumed on this planet in one year ($4.1 \times 10^{20}$ J). As an intermittent energy source (night and day), there is no way to store this enormous amount of electricity each day to be used during the night. It is well known that many households with solar panels do not have an adequate method of storing their unused power. Batteries give the option of storing limited amounts of energy, but suffer from finite lifetimes and contain significantly toxic chemicals that are difficult to dispose of. Also, there are huge losses associated with transporting electricity over large distances. Therefore, a method of storing the sun's energy in chemical bonds then releasing it without harmful byproducts is indeed the "Holy Grail" in solar energy conversion[1,2].

**Surface Plasmon Resonance:** Plasmons are the collective oscillation of the free charge in a conducting material. Light below the plasma frequency is reflected because the electrons in the metal screen the electric field of the light. Light above the plasma frequency is transmitted because the electrons cannot respond fast enough to screen it. Surface plasmons are oscillations confined to the surfaces of conducting materials and interact strongly with light. A resonance in the absorption occurs at the plasmon frequency when the real part of the dielectric function goes to zero. Irradiating metal nanoparticles with light at their plasmon frequency generates intense electric fields at the surface of the nanoparticles, as shown in Figure 1. The frequency of this resonance can be tuned by varying the nanoparticle size, shape, material, and proximity to other nanoparticles[3]. For example, the plasmon resonance of silver, which lies in the UV, can be shifted into the visible range by making the nanoparticle size very small. Similarly, the plasmon resonance of gold in the visible range can be brought into the infrared wavelength range by minimizing the nanoparticle size. Nurmikko and others have fabricated arrays of nanoparticles with different spacing using electron beam lithography[3,4]. Their optical measurements show that the plasmon resonance increases asymptotically as the particles are brought closer together. This was corroborated by the calculations of Schatz et al. using an interacting dipole model that showed the plasmonic resonance to be $10^3$ times stronger between two nearly touching nanoparticles[5]. The intense electric fields produced near plasmon resonant metallic nanoparticles are currently utilized in surface enhanced Raman spectroscopy (SERS) to produce enhancement factors as high as $10^{14}$ [6-8]. Numerical simulations have predicted SERS enhancement factors up to $10^{10}$ [9,10].

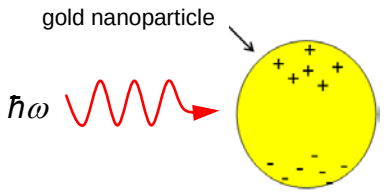


**Figure 1.** Schematic diagram of surface plasmon excitation.

**Metal Oxide Catalysis:** Metal oxides (e.g., $TiO_2$, $Fe_2O_3$, PbO) are promising photocatalysts for a number of applications, including solar fuel production, oxidation of pollutants, and anti-fogging/self-cleaning coatings for windows and lenses. As a self-cleaning catalyst, $TiO_2$ does not suffer from the corrosion problems associated with photovoltaic cells. Fujishima and Honda first demonstrated the photochemical splitting of water on *n*-type $TiO_2$ electrodes using UV light[11]. The absorption of light is necessary to initiate the charge transfer mechanism of the catalytic process, as shown below in Figure 2. In $TiO_2$, an absorbed photon creates an electron-hole pair. The electron drives a reduction of the $H^+$ ions to produce $H_2$ gas, while the holes drive the oxidation of the $OH^-$ ions, producing $O_2$ gas. While $TiO_2$ is one of the most promising photocatalysts, it does not absorb light in the visible region of the electromagnetic spectrum. Figure 3 shows this problem graphically with the absorption spectrum of $TiO_2$ superimposed over the solar spectrum[12]. Because of $TiO_2$'s short wavelength cutoff, there are very few solar photons (~4%) that can be used to drive this photocatalyst. Several attempts to extend the cutoff wavelength of this material have resulted in only slightly improved efficiencies[13]. In this proposal, we explore a new

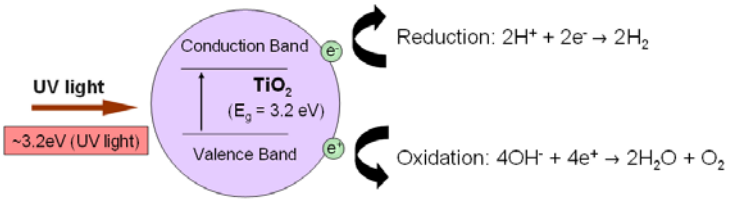


**Figure 2.** Schematic diagram illustrating the photochemical oxidation and reduction processes of $TiO_2$.

mechanism for inducing increased amounts of charge in $TiO_2$ films by exploiting the extremely large plasmon resonance of Au and Ag nanoparticles. The large electric fields produced on the surface of metal nanoparticles can be used to induce charge in the $TiO_2$ catalyst necessary to drive the catalytic reaction. By using a combination of different nanoparticle sizes, the absorption spectrum, and hence the photocatalytic activity, can be tailored to match the solar spectral radiance. Tian et al. have observed enhanced photocatalytic oxidation of ethanol and methanol in $TiO_2$ films loaded with gold nanoparticles[14]. While these results were attributed to charge transfer from the nanoparticles to the metal oxide, the details of this mechanism are not fully understood. In the work carried out under this award, we have investigated the energy and charge transfer dynamics systematically using well-defined sample geometries, as described below.

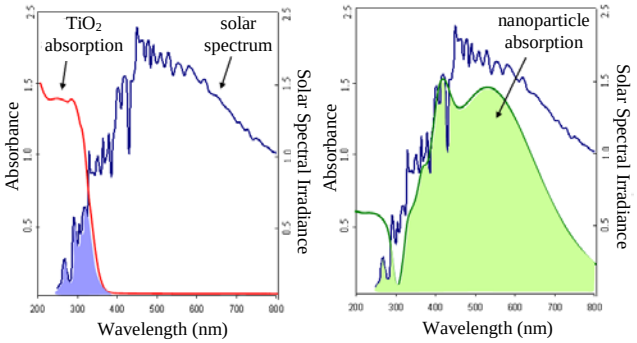


**Figure 3.** Solar spectral radiance and absorption spectrum of $TiO_2$ (left) and plasmonic nanoparticles (right).

## MAIN FINDINGS

By integrating strongly plasmonic metal nanostructures with strongly catalytic metal oxide semiconductors, we have demonstrated enhancement of 1.) photocatalytic water splitting, 2.) photo-decomposition of organic compounds, 3.) CO oxidation, and 4.) photo-reduction of $CO_2$ to form methane and other hydrocarbons. Below, we describe these results in more detail.

**1.) Photocatalytic Water Splitting:** Photocatalytic water splitting has been of great interest since the early 1970s, after the first demonstration by Fujishima and Honda under ultraviolet radiation[15]. As mentioned above, $TiO_2$ is one of the most promising photocatalysts; however, it does not absorb light in the visible region of the electromagnetic spectrum. Through plasmonic enhancement, we have demonstrated a new mechanism for inducing increased amounts of charge in $TiO_2$ films by exploiting the extremely large plasmon resonance of Au nanoparticles[16]. As shown schematically in Figure 4a, the photocatalytic reaction rates of $TiO_2$ with and without Au nanoparticles are measured in a 1M KOH solution using a three-terminal potentiostat, with the $TiO_2$ film, a Ag/AgCl electrode, and a graphite electrode functioning as the working, reference, and counter electrodes, respectively. The $TiO_2$ film is irradiated in a sealed quartz flask, while the generated gas is monitored by mass spectrometry, verifying the production of $H_2$ under illumination, as shown in Figure 4b. Figures 4c and 4d show the photocurrents induced in $TiO_2$ with and without plasmonic Au nanoparticles under visible illumination. This photocurrent provides a good measure of the reaction rate, since every two electrons in this reaction produces one hydrogen molecule[16]. This light (532nm and 633nm) is well below the bandgap of this material; however, due to defect and impurities, we observe a finite photocurrent for this material in the visible range. By comparing the photocurrents for $TiO_2$ with (dashed) and without (solid) gold nanoparticles, we see a 5-fold increase in the reaction rate with the addition of Au nanoparticles at 532nm

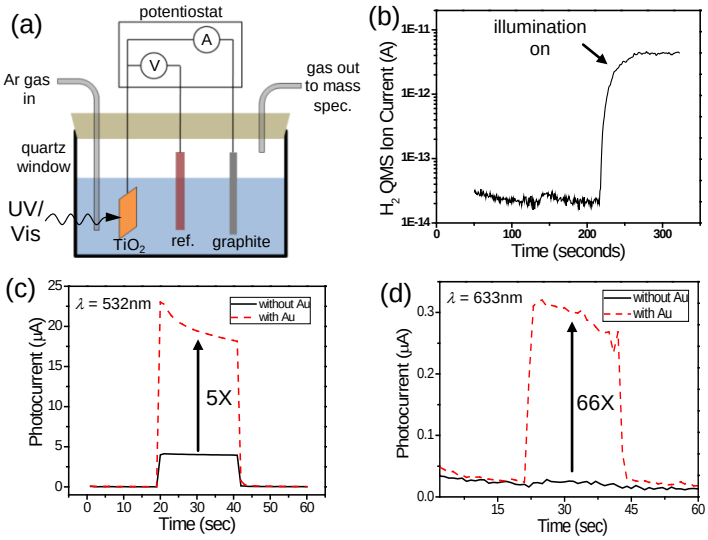


**Figure 4.** (a) Schematic diagram, (b) quadrupole mass spectrometer data, and (c,d) photocurrents observed in plasmon enhanced $TiO_2$ under visible illumination.

and a 66-fold increase at 633nm. The slight transient seen in Figure 4c is the commonly seen trapped surface charge that is released upon irradiation[43].

**Spectral Response of the Photocatalytic Activity:** In addition to the fixed wavelength lasers and UV light source used in our preliminary results, we have also measured the spectral response of the photocatalytic activity to provide a quantitative basis for determining the precise mechanism underlying the observed catalytic enhancement. Here, we use a recently acquired Fianium supercontinuum white light laser source in conjunction with a Princeton Instruments double grating monochromator to provide extinction spectra over the 400-1600nm wavelength range[17]. Figure 13a shows the photocurrent spectra of anodic $TiO_2$ with and without Au nanoparticles. Both samples show an appreciable photocurrent for wavelengths below 500nm. An enhancement in the photocurrent of $TiO_2$ with Au nanoparticles (Figure 13b) can be seen for wavelengths above 500nm, with a maximum enhancement occurring around 650nm, which is consistent with the plasmon resonance frequency.

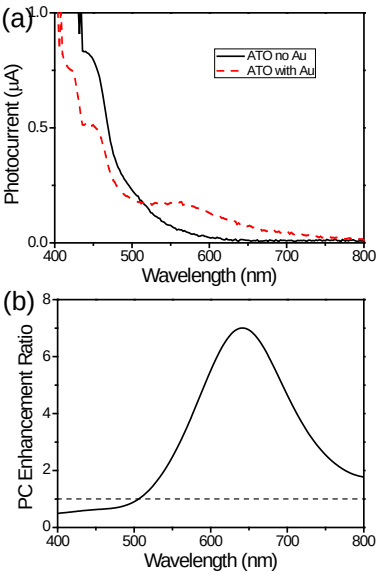


**Figure 13.** (a) Photocurrent spectrum of anodic $TiO_2$ with and without Au. (b) Photocurrent enhancement ratio.

**Sample Preparation:** We prepare $TiO_2$ in the anatase crystalline phase by electrochemically oxidizing titanium foils in an ethylene glycol electrolyte containing 0.25 wt% $NH_4F$ and 2% wt $H_2O$ at an anodization potential of 30 V for two hours, using a graphite rod as the cathode[18]. A gold film with a nominal thickness of 5nm is then evaporated on the surface of the $TiO_2$. This thin gold film is known to form island-like growth that is strongly plasmonic and serves as a good substrate for surface enhanced Raman spectroscopy (SERS)[8,19].

**Electromagnetic Simulations:** In order to understand the underlying mechanism of catalytic enhancement, we perform numerical simulations of the electromagnetic response of these plasmonic Au nanoparticles using the finite-difference time-domain (FDTD) method, carried out on USC's multi-teraflop supercomputing facility. Figure 5a shows a scanning electron microscope (SEM) image of a gold nanoparticle-island film deposited on top of anodic $TiO_2$. The electromagnetic response of this film, as shown in Figures 5b-d, is dominated by local "hot spots" (bright yellow) that can be seen between nearly touching Au nanoparticles. This is a well-known phenomenon in plasmonics and has been demonstrated by several research groups[9,20,21]. Figure 5d shows a cross-sectional plot of the electric field distribution of one of these hot-spot regions in the *z*-dimension. In this hot-spot region, the electric field intensity at the $TiO_2$ surface reaches 1000 times that of the incident electric field intensity. This means that the photoabsorption (and hence electron-hole pair generation) rate is 1000 times higher than that of the incident electromagnetic radiation. This is particularly advantageous considering the small crystal grain sizes and high defect concentrations in anodic $TiO_2$, which limit the exciton diffusion length to ~10nm[22-24]. As a result, only photons absorbed within 10nm of the $TiO_2$ surface will contribute to the photocatalytic splitting of water. Here, the plasmonic nanoparticles couple light very effectively from the far-field to the near-field at the $TiO_2$ surface. Consequently, most of the photogenerated charge created by the plasmon excitation will contribute to the surface catalysis (water splitting).

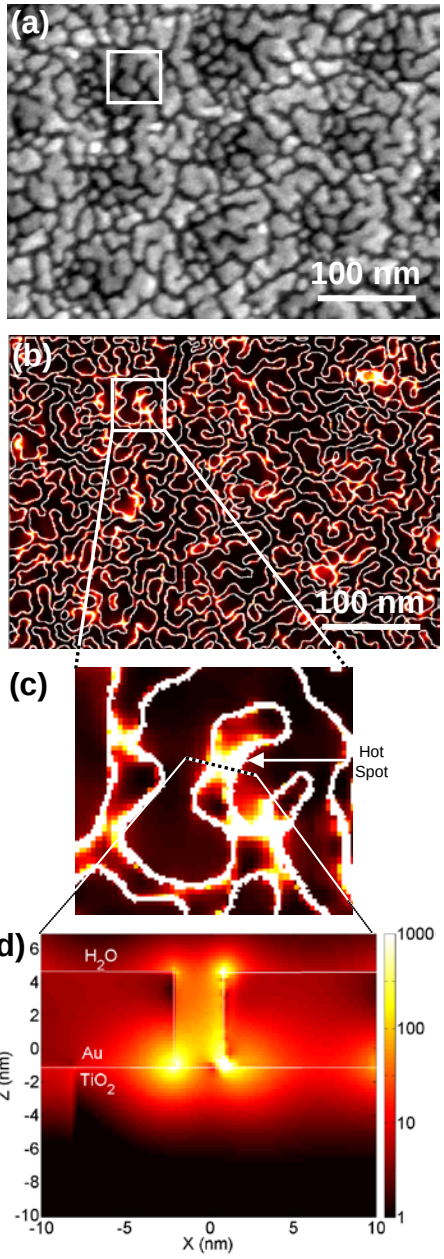


**Figure 5.** (a) SEM image of 5 nm Au island film on $TiO_2$. (b-d) Electric field intensity at the interface of Au–$TiO_2$ at the resonance calculated using FDTD.

We can calculate the photocatalytic enhancement factor based on the results of the FDTD simulation. Since the photon absorption rate is proportional to the electric field squared ($|E|^2$), we integrate $|E|^2$ over the whole film and divide by the integral of the incident electromagnetic field squared ($|E_o|^2$), as shown in Eq. 1 below. In the *z*-dimension, we integrate only from the $TiO_2$ surface ($z$ = 0) to one exciton diffusion length below the surface ($z$ = -10nm). The value for the EF when integrating over the whole simulation area (400 nm × 300 nm) is 12X, which is consistent with the values observed experimentally. It should be noted, however, that this value is for this random distribution of gold islands that is not optimized geometrically. If, instead, we integrate only over the area of one hot spot, as shown in Figure 5c, an EF of 190X would result. Given the very small fraction of the total catalytic surface area comprising these hot-spot regions, it is remarkable that we still observe a net improvement in the photocatalytic water splitting with the addition of gold nanoparticles. We, therefore, believe that enhancement factors many times larger than this are possible if this plasmonic film can be optimized to make more efficient use of the total surface area. The use of metal nanoparticles to enhance light absorption and photocurrents in solar cells has been reported using a similar plasmonic coupling mechanism. Here, we utilize the plasmonic field enhancement to improve $TiO_2$ photocatalysis in the visible wavelength range.

$$EF = \frac{\int_{-10\,\mathrm{nm}}^{0} dz \int dxdy|E|^2}{\int_{-10\,\mathrm{nm}}^{0} dz \int dxdy|E_o|^2} \quad (1)$$

**2.) Photocatalytic Decomposition of Methyl Orange:** In addition to water splitting, we have demonstrated photocatalytic decomposition of the organic dye molecule, methyl orange (MO)[25]. In this photocatalytic decomposition process, the electrons created in the $TiO_2$ conduction band reduce the $O_2$, the hole in the valence band oxidizes the OH ion, and these free radicals then break down the MO molecule. The photocatalytic decomposition of organic molecules is of great interest for the removal of pollutants from water and air. Semiconductor photocatalysts (e.g., $TiO_2$, ZnO, SnO, $In_2O_3$) have been shown to effectively catalyze the decomposition of many pollutants[26-28]. While $TiO_2$ is one of the most promising photocatalysts for this purpose[28-30], its short wavelength cutoff prohibits the use of solar photons to drive these processes. Several attempts have been made to extend the cutoff wavelength of this catalyst, including doping[26,31,32] and defect creation[33,34]. However, these have only extended the absorption edge of $TiO_2$ to approximately 420 nm.

Using the same Au nanoparticle/$TiO_2$ substrates described above for water splitting, we have demonstrated significant enhancement in the photocatalytic decomposition of methyl orange under visible illumination. Here, we quantify the reaction rate by monitoring changes in the optical (UV-Vis) absorption of the dye molecule itself, rather than the photocurrent. Under visible illumination (532nm) for 1 hour, bare $TiO_2$ shows a 1.4% drop in methyl orange density, while the $TiO_2$ with Au nanoparticles shows a 13% drop in density. This corresponds to a 9-fold enhancement in the photocatalytic decomposition rate through plasmon excitation. All the necessary control experiments have been performed to establish that this catalytic enhancement is due to the intimate interaction between these two materials and can be attributed to the plasmon resonance of the Au nanoparticles.

**3.) Plasmon Resonant Enhancement of Carbon Monoxide Catalysis:** In addition to the photoelectrochemical processes described above ($H_2O$ splitting and MO decomposition), we have also demonstrated plasmonic enhancement of a thermally driven catalytic reaction, namely carbon monoxide oxidation. The catalytic conversion of CO to $CO_2$ represents a simple reaction system with small molecules and well-understood pathways. In this gas phase reaction, we irradiate photocatalysts consisting of Au nanoparticles on $Fe_2O_3$ supports, while monitoring the reaction rate using mass spectrometry[35]. Figure 6 shows the mass spectrometer signals of $CO_2$ plotted during a 5-second laser exposure (48mW at a wavelength of 532nm). Here, we observe a rapid increase in the $CO_2$ concentration when the laser is incident on the $Fe_2O_3$-Au nanoparticle composite. However, when Au nanoparticles are irradiated alone with no $Fe_2O_3$, no change in the $CO_2$ signal is observed, as shown in Figure 6. Similarly, when we irradiate $Fe_2O_3$ alone with no Au nanoparticles, we observe no production of $CO_2$. We, therefore, conclude that this reaction is not driven solely by the thermal (plasmonic) heating of the gold nanoparticles, but relies intimately on the interaction of these two materials. A comparison of the plasmonically driven catalytic reaction rate with that obtained under uniform heating is shown in Figure 6b. The data shows that the laser-induced catalysis is at least 2-3 orders of magnitude higher than that of uniform heating. Here, we believe that the localized plasmonic heating of the nanoparticles creates large temperature gradients, enabling the controlled condensation of reverse reaction byproducts, which in turn allows the desired reaction to be driven forward more efficiently.

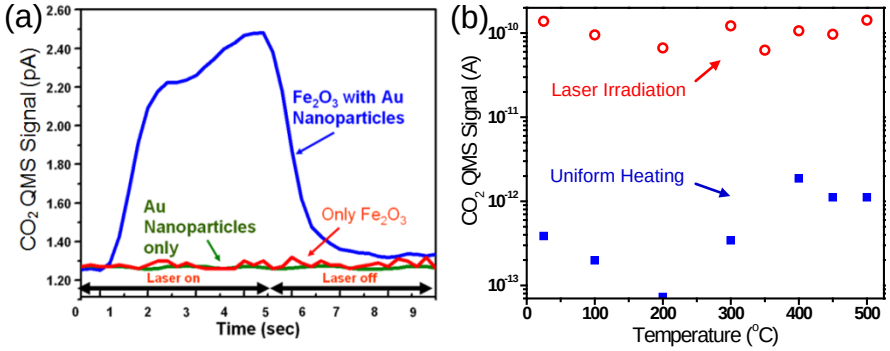


**Figure 6.** (a) Quadropole mass spectrometer signals for $CO_2$ during 5 sec laser-induced reactions. (b) Comparison of the average $CO_2$ QMS signal for laser irradiation and uniform heating.

**4.) Photocatalytic Methane Formation:** In our primary reaction of interest, we have studied the photocatalytic production of methane by the reduction of $CO_2$ by $H_2O$: $CO_2 + 2H_2O \rightarrow CH_4 + 2O_2$.

Methane formation is a somewhat more complicated process than water splitting, involving the following half-reactions:

$$2H_2O + 4h^+ \rightarrow O_2 + 4H^+ \qquad (4)$$

$$CO_2 + 8H^+ + 8e^- \rightarrow CH_4 + 2H_2O \qquad (5)$$

The free energy for the overall methane formation reaction

$$CO_2 + 2H_2O\ (g) \rightarrow CH_4 + 2O_2 \qquad (6)$$

is 1137 kJ/mol; a process requiring 8 photons. Here, we build upon the previous work of Varghese et al., who have achieved high photoconversion efficiencies on copper and platinum-loaded titania nanotubes under solar illumination[36]. Considering only the solar photons above the $TiO_2$ bandgap (3.2eV), they report photoconversion efficiencies of 16.25%. Again, we aim to extend this photocatalysis into the visible range by inducing charge in the $TiO_2$ through the plasmon resonance phenomenon. In addition to $CH_4$, the reduction of $CO_2$ by $H_2O$ can produce other hydrocarbons, including HCHO and $CH_3OH$.

Figure 8a shows the conduction band (CB) and valence band (VB) of $TiO_2$ together with the redox potentials of $CO_2$ for the three reduction byproducts: $CH_4$, HCHO, and $CH_3OH$. Since the conduction band of the $TiO_2$ lies above the reduction potential of the byproducts, the injection of electrons from $TiO_2$ to initiate the reduction of $CO_2$ with $H_2O$ is energetically favorable. Figure 8b shows the gas chromatography (GC) signals of photocatalysis under UV irradiation ($\lambda$ = 254nm) for three catalytic substrates: $TiO_2$, Au, and Au/$TiO_2$. Here, photocatalytic production of $CH_4$, $C_2H_6$, HCHO, and $CH_3OH$ can be seen in the data. Methane production is dominant because its reduction potential is significantly lower than the $TiO_2$ conduction band, and hence more favorable energetically. In Figure 8c, we plot the catalytic yield of $CH_4$ under visible illumination (532nm) for the three catalytic substrates: $TiO_2$, Au, and Au/$TiO_2$. Under visible illumination (Figure 8c), we only observe reduction of $CO_2$ for the

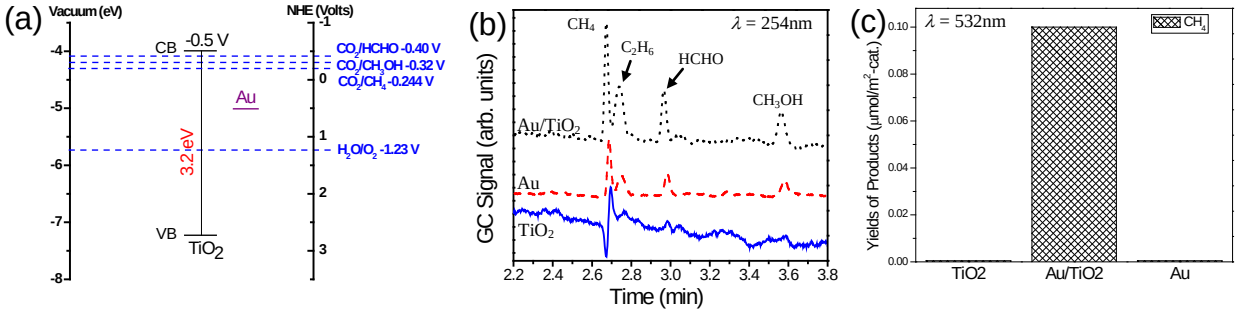


**Figure 8.** (a) Energy band alignment of anatase $TiO_2$ together with the work function of Au and relevant redox potentials of $CO_2$ and $H_2O$. GC signals for Au, $TiO_2$, and Au/$TiO_2$ catalysts under (b) UV illumination and (c) visible illumination.

Au/$TiO_2$ catalyst, and with this catalyst, we observe only the $CH_4$ byproduct. This implies this photocatalyst is more selective under visible illumination than bare $TiO_2$ under UV illumination, most likely due to fewer over-energetic electrons. This data shows an enhancement factor of at least 100X, as limited by the detector sensitivity.

**Fabricating Well-Defined Plasmon Resonant Nanostructures**

In addition to the four reaction systems discussed above, we have also developed a method for fabricating strongly plasmonic metal nanoparticles arrays with 1-2nm separation. In the plasmon-enhanced reactions described above, samples consisted of randomly distributed Au islands (or nanoparticles) (see Figure 5a) deposited on top of $TiO_2$. Larger catalytic enhancement factors are expected by precisely controlling the metal nanoparticle size, shape, and separation.

**Electron Beam Lithography:** While several methods exist for creating surface plasmon resonant nanostructures[3,8,37-40], electron beam lithography (EBL) provides the most precise control over nanostructure geometry, including an extensive range of size, shape, separation, and material. In particular, EBL provides a means of accurately studying coupled plasmonic systems, which are more strongly resonant than individual nanoparticles. The aim of this work is to use EBL to identify optimized nanostructures that can subsequently be mass-produced with low-cost nanoimprint lithography or self-assembly techniques, as described below. Figure 9 shows scanning electron microscope (SEM) images of several Au nanoparticle arrays with various geometries fabricated using electron beam lithography. These

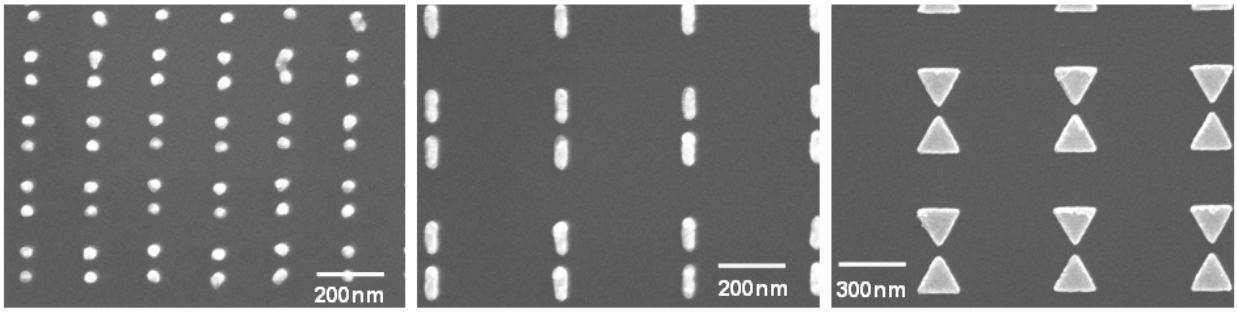


**Figure 9.** Au nanostructure arrays with various geometries fabricated by electron beam lithography and measured at USC.

arrays were generated using a 100 kV electron beam with a 60 μm aperture in a bi-level MMA/PMMA resist. Using this technique, we can generate hundreds of different patterns on a single chip, allowing us to perform a systematic study over all of the geometric variables including size, shape, spacing, and materials.

**1nm Particle Separation:** From numerical electrodynamics calculations, the largest plasmonic electric fields are achieved between two nearly touching nanoparticles[9,10,41]. Since this separation is one order of magnitude smaller than that which can be reliably produced with the best electron beam lithography, we have developed a new method using angle evaporation to controllably create 0.5 to 2nm nanogaps[42]. The scheme uses a double layer of poly methyl methacrylate (PMMA) on methyl methacrylate (MMA) resist, which enables the preferential exposure of the more sensitive MMA layer, leaving a free-standing PMMA mask, as shown in Figure 10a. In patterning the nanogaps, a thin layer of metal (e.g., Au or Ag) is first deposited at normal incidence. The sample is then rotated by a small angle (~$10^o$) and a second layer of metal is deposited. The size of the nanogap is determined by the angle of the second evaporation, $\theta$, and the thickness of the first evaporation, $t_1$, and is given by $t_1 \cdot \tan\theta$. An angle of $\theta = 10^o$ and thickness of $t_1 = 10$nm will yield a gap of 1.8nm. By decreasing the angle of evaporation to $\theta = 5^o$, the gap size is reduced to 0.87nm. Figure 10b shows high resolution transmission electron microscopy (HRTEM) images of an array of gold nanoparticles created by this angle evaporation technique[42]. Figure 10c shows a high-magnification image of one nanoparticle pair exhibiting a 2nm gap. This dimer was fabricated with $t_1 = 25$nm and $\theta = 5°$, which is consistent with the 2nm gap observed by HRTEM, based on the trigonometric formula $t_1 \cdot \tan\theta$. The electric field enhancement between these two nanoparticles exceeds $10^4$ times the incident electric field intensity, as shown in the FDTD simulation of Figure 17 below.

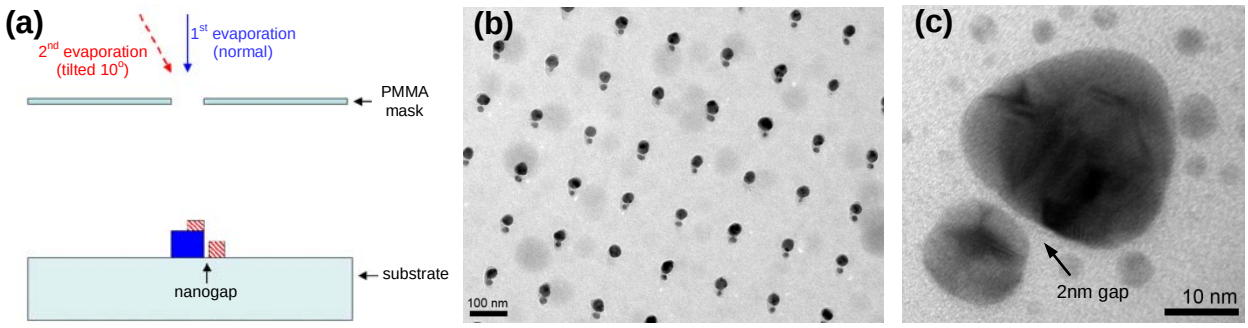


**Figure 10.** (a) Schematic diagram of the angle evaporation technique for fabricating nm-size gaps in a controlled manner. (b) Low and (c) high magnification TEM images of gold nanoparticles with 2nm gaps fabricated using the angle evaporation technique.

**FDTD Simulation based on HRTEM Images:** The HRTEM images shown in Figures 10b, 10c, and 17a were taken in a Joel JEM-2100F advanced field emission transmission electron microscope. This system operates at voltages up to 200kV, producing a point-to-point resolution of 0.14nm. These nearly touching nanoparticles were fabricated on 50nm thick SiN membranes (SPI, Inc.), which are transparent to high energy electron radiation, enabling HRTEM to be performed. We have simulated the electromagnetic response of this dimer by defining the spatial extent of the metal nanoparticles from this high resolution TEM image. Figure 17b shows the electric field intensity distribution of this gold nanoparticle dimer, irradiated at normal incidence at the plasmon resonance frequency[42]. This is a full, 3D FDTD simulation entailing 50 million grid points, 200,000 time steps, a grid size of 2Å, and several hours of computation time on the supercomputing facility at USC. Here, the maximum electric field intensity lies in the gap between the nanoparticles, with a value 35,000 times that of the incident field intensity. Repeating this calculation with Ag instead of Au yielded an even larger enhancement factor.

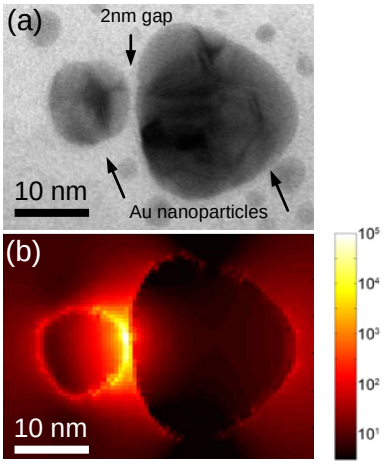


**Figure 17.** (a) HRTEM image and (b) FDTD simulation of nearly touching Au nanoparticles.

## CONCLUSION

We have demonstrated photocatalytic enhancement in four different reaction systems by integrating strongly plasmonic metal nanostructures with strongly catalytic metal oxide semiconductors. Through numerical simulations, we have identified the mechanism underlying this enhancement, which is based on the local electric field enhancement rather than the direct transfer of charge between the plasmonic and catalytic materials. While these results demonstrate proof-of-principle of plasmonic enhancement of photocatalysis, further investigation is needed in order to optimize this process and to address several questions that remain open regarding the precise mechanism underlying this catalytic enhancement.

**References Cited**


1. Bard, A.J. and Fox, M.A., "Artificial Photosynthesis - solar splitting of water to hydrogen and oxygen." *Accounts of Chemical Research*, **28**, 141-145 (1995).
2. Eisenberg, R. and Gray, H.B., "Preface on making oxygen." *Inorganic Chemistry*, **47**, 1697-1699 (2008).
3. Atay, T., Song, J.H., and Nurmikko, A.V., "Strongly interacting plasmon nanoparticle pairs: From dipole-dipole interaction to conductively coupled regime." *Nano Letters*, **4**, 1627-1631 (2004).
4. Su, K.H., Wei, Q.H., Zhang, X., Mock, J.J., Smith, D.R., and Schultz, S., "Interparticle coupling effects on plasmon resonances of nanogold particles." *Nano Letters*, **3**, 1087-1090 (2003).
5. Zou, S.L. and Schatz, G.C., "Silver nanoparticle array structures that produce giant enhancements in electromagnetic fields." *Chemical Physics Letters*, **403**, 62-67 (2005).
6. Kneipp, K., Wang, Y., Kneipp, H., Perelman, L.T., Itzkan, I., Dasari, R., and Feld, M.S., "Single molecule detection using surface-enhanced Raman scattering (SERS)." *Physical Review Letters*, **78**, 1667-1670 (1997).
7. Kneipp, K., Kneipp, H., Corio, P., Brown, S.D.M., Shafer, K., Motz, J., Perelman, L.T., Hanlon, E.B., Marucci, A., Dresselhaus, G., and Dresselhaus, M.S., "Surface-enhanced and normal Stokes and anti-Stokes Raman spectroscopy of single-walled carbon nanotubes." *Physical Review Letters*, **84**, 3470-3473 (2000).
8. Kumar, R., Zhou, H., and Cronin, S.B., "Surface-enhanced Raman spectroscopy and correlated scanning electron microscopy of individual carbon nanotubes." *Applied Physics Letters*, **91**, 223105 (2007).
9. Oubre, C. and Nordlander, P., "Finite-difference Time-domain Studies of the Optical Properties of Nanoshell Dimers." *J. Phys. Chem. B*, **109**, 10042 (2005).
10. Nordlander, P., Oubre, C., Prodan, E., Li, K., and Stockman, M.I., "Plasmon Hybridization in Nanoparticle Dimers." *Nano Letters*, **5**, 899 (2004).
11. Fujishim.A and Honda, K., "Electrochemical Photolysis of Water at a Semiconductor Electrode." *Nature*, **238**, 37 (1972).
12. Seinfeld, J.H. and Pandis, S.N., *Atmospheric Chemistry and Physics*. 1998, New York, Chichester, Brisbane, Singapore, Toronto: John Wiley & Sons, Inc.
13. Khan, S.U.M., Al-Shahry, M., and Ingler, W.B., "Efficient photochemical water splitting by a chemically modified *n*-$TiO_2$." *Science*, **297**, 2243-2245 (2002).
14. Tian, Y. and Tatsuma, T., "Mechanisms and applications of plasmon-induced charge separation at $TiO_2$ films loaded with gold nanoparticles." *Journal of the American Chemical Society*, **127**, 7632-7637 (2005).
15. Fujishima. A and Honda, K., "Electrochemical Photolysis of Water at a Semiconductor Electrode." *Nature*, **238**, 37 (1972).
16. Liu, Z., Hu, W., Pavaskar, P., Aykol, M., and Cronin, S.B., "Plasmon Resonant Enhancement of Photocatalytic Water Splitting." *J. Phys. Chem.*, submitted (2010).
17. Jensen, T.R., Malinsky, M.D., Haynes, C.L., and Van Duyne, R.P., "Nanosphere lithography: Tunable localized surface plasmon resonance spectra of silver nanoparticles." *Journal of Physical Chemistry B*, **104**, 10549-10556 (2000).
18. Grimes, C.A., "Synthesis and application of highly ordered arrays of $TiO_2$ nanotubes." *J. Mater. Chem.*, **17**, 1451-1457 (2007).

19. Duyne, R.P.V., Hulteen, J.C., and Treichel, D.A., "Atomic force microscopy and surface-enhanced Raman spectroscopy. I. Ag island films and Ag film over polymer nanosphere surfaces supported on glass." *J. Chem. Phys*, **99**, 2101-2115 (1993).
20. Hao, E. and Schatz, G.C., "Electromagnetic fields around silver nanoparticles and dimers." *Journal of Chemical Physics*, **120**, 357 (2003).
21. Jiang, J., Bosnick, K., Maillard, M., and Brus, L., "Single molecule Raman spectroscopy at the junctions of large Ag nanocrystals." *J. Phys. Chem. B*, **107**, 9964 (2003).
22. Leng, W.H., Barnes, P.R.F., Juozapavicius, M., O'Regan, B.C., and Durrant, J.R., "Electron Diffusion Length in Mesoporous Nanocrystalline $TiO_2$ Photoelectrodes during Water Oxidation." *Journal of Physical Chemistry Letters*, **1**, 967-972 (2010).
23. Savenije, T.J., Warman, J.M., and Goossens, A., "Visible light sensitization of titanium dioxide using a phenylene vinylene polymer." *Chemical Physics Letters*, **287**, 148-153 (1998).
24. Arango, A.C., Johnson, L.R., Bliznyuk, V.N., Schlesinger, Z., Carter, S.A., and Horhold, H.H., "Efficient titanium oxide/conjugated polymer photovoltaics for solar energy conversion." *Advanced Materials*, **12**, 1689 (2000).
25. Hou, W., Liu, Z., Pavaskar, P., Hung, W.H., and Cronin, S.B., "Plasmonic Enhancement of Photocatalytic Decomposition of Methyl Orange under Visible Light." *J. Catal.*, submitted (2010).
26. Wang, X.H., Li, J.G., Kamiyama, H., Moriyoshi, Y., and Ishigaki, T., "Wavelength-sensitive photocatalytic degradation of methyl orange in aqueous suspension over iron(III)-doped $TiO_2$ nanopowders under UV and visible light irradiation." *J. Phys. Chem. B*, **110**, 6804-6809 (2006).
27. Kislov, N., Lahiri, J., Verma, H., Goswami, D.Y., Stefanakos, E., and Batzill, M., "Photocatalytic Degradation of Methyl Orange over Single Crystalline ZnO: Orientation Dependence of Photoactivity and Photostability of ZnO." *Langmuir*, **25**, 3310-3315 (2009).
28. Talebian, N. and Nilforoushan, M.R., "Comparative study of the structural, optical and photocatalytic properties of semiconductor metal oxides toward degradation of methylene blue." *Thin Solid Films*, **518**, 2210-2215 (2010).
29. Wang, Z.H., Jiang, T.S., Du, Y.M., Chen, K.M., and Yin, H.B., "Synthesis of mesoporous titania and the photocatalytic activity for decomposition of methyl orange." *Mater. Lett.*, **60**, 2493-2496 (2006).
30. Wu, C.H. and Chern, J.M., "Kinetics of photocatalytic decomposition of methylene blue." *Ind. Eng. Chem. Res.*, **45**, 6450-6457 (2006).
31. Sajjad, A.K.L., Shamaila, S., Tian, B.Z., Chen, F., and Zhang, J.L., "Comparative studies of operational parameters of degradation of azo dyes in visible light by highly efficient $WO_x/TiO_2$ photocatalyst." *J. Hazard. Mater.* , **177**, 781-791 (2010).
32. Shamaila, S., Sajjad, A.K.L., Chen, F., and Zhang, J.L., "Study on highly visible light active $Bi_2O_3$ loaded ordered mesoporous titania." *Appl. Catal. B: Environ.*, **94**, 272-280 (2010).
33. Takeuchi, M., Yamashita, H., Matsuoka, M., Anpo, M., Hirao, T., Itoh, N., and Iwamoto, N., "Photocatalytic decomposition of NO under visible light irradiation on the Cr-ion-implanted $TiO_2$ thin film photocatalyst." *Catal. Lett.*, **67**, 135-137 (2000).

34. Takeuchi, M., Yamashita, H., Matsuoka, M., Anpo, M., Hirao, T., Itoh, N., and Iwamoto, N., "Photocatalytic decomposition of NO on titanium oxide thin film photocatalysts prepared by an ionized cluster beam technique." *Catal. Lett.*, **66**, 185-187 (2000).
35. Hung, W.H., Aykol, M., Valley, D., Hou, W.B., and Cronin, S.B., "Plasmon Resonant Enhancement of Carbon Monoxide Catalysis." *Nano Letters*, **10**, 1314-1318 (2010).
36. Varghese, O.K., Paulose, M., LaTempa, T.J., and Grimes, C.A., "High-Rate Solar Photocatalytic Conversion of $CO_2$ and Water Vapor to Hydrocarbon Fuels." *Nano Letters*, **9**, 731-737 (2009).
37. Hicks, E.M., Zhang, X.Y., Zou, S.L., Lyandres, O., Spears, K.G., Schatz, G.C., and Van Duyne, R.P., "Plasmonic properties of film over nanowell surfaces fabricated by nanosphere lithography." *Journal of Physical Chemistry B*, **109**, 22351-22358 (2005).
38. Van Duyne, R.P., Hulteen, J.C., and Treichel, D.A., "Atomic-force microscopy and surface-enhanced Raman spectroscopy. I. Ag island films over polymer nanosphere surfaces supported on glass." *Journal of Chemical Physics*, **99**, 2101-2115 (1993).
39. Jaramillo, T.F., Baeck, S.H., Cuenya, B.R., and McFarland, E.W., "Catalytic activity of supported Au nanoparticles deposited from block copolymer micelles." *Journal of the American Chemical Society*, **125**, 7148-7149 (2003).
40. Meltzer, S., Resch, R., Koel, B.E., Thompson, M.E., Madhukar, A., Requicha, A.A.G., and Will, P., "Fabrication of nanostructures by hydroxylamine seeding of gold nanoparticle templates." *Langmuir*, **17**, 1713-1718 (2001).
41. Pavaskar, P. and Cronin, S.B., "Iterative optimization of plasmon resonant nanostructures." *Applied Physics Letters*, **94**, 253102 (2009).
42. Theiss, J., Pavaskar, P., Echternach, P.M., Muller, R.E., and Cronin, S.B., "Plasmonic Nanoparticle Arrays with Nanometer Separation for High-Performance SERS Substrates." *Nano Letters*, **10**, 2749 (2010).